Available online at www.sciencedirect.com
ScienceDirect
Proceedings of the Combustion Institute 35 (2015) 679–686
Proceedings of the Combustion Institute
www.elsevier.com/locate/proci

Comparative study on the laminar flame speed enhancement of methane with ethane and ethylene addition

S. Ravi [*], T.G. Sikes, A. Morones, C.L. Keesee, E.L. Petersen

Department of Mechanical Engineering, Texas A&M University, College Station, TX 77843, USA

Available online 26 June 2014

Abstract

A systematic analysis of the flame speed enhancement effects of ethane and ethylene addition to methane was performed. Flame speeds of outwardly propagating spherical flames were measured in a high-pressure, cylindrical flame speed vessel using schlieren photography. It was ensured that the measured data were outside the ignition- and chamber-confinement-affected radii. The unstretched, unburnt flame speeds were obtained using nonlinear extrapolation methods from the experimentally determined stretched flame speeds. The AramcoMech 1.3 kinetics mechanism was validated against flame speeds of ethane, ethylene, and acetylene over a wide range of pressures and equivalence ratios. Good agreement between the measured data and those reported in the literature was seen. The model agreed closely with the measurements at fuel-lean conditions, but a slight over prediction was observed for the fuel-rich cases. Flame speeds of 80/20 and 60/40 (by volume) CH_4/C_2H_x mixtures in air and in air with excess nitrogen were measured over a wide range of fuel concentrations. In all cases, the addition of ethylene increased the flame speed more than did an equivalent addition of ethane. The Arrhenius effect (predominantly kinetic effect) was the principal driver for flame speed enhancement of methane with ethane/ethylene addition. Sensitivity analysis revealed that thermal and diffusive pathways were equally contributing to the flame speed enhancement of CH_4/C_2H_6 mixtures, but the latter played a comparatively minor role in the C_2H_4-based blends.

© 2014 The Combustion Institute. Published by Elsevier Inc. All rights reserved.

Keywords: Fuel blends; Laminar flame speeds; Ethane; Ethylene; Acetylene

---

1. Introduction

Laminar flame speed is not only a fundamental property of a fuel, but it is also a convenient tool for validating chemical kinetics mechanisms. Ethylene (C_2H_4) is an important intermediate species in the oxidation of ethane [1] and higher-order hydrocarbons (HC) used as surrogates for biofuels [2]. Furthermore, ethylene was shown to

---

[*] Corresponding author. Address: Texas A&M University, Department of Mechanical Engineering, College Station, TX 77843-3123, USA. Fax: +1 (979) 845 3081.
E-mail address: sri327@gmail.com (S. Ravi).

http://dx.doi.org/10.1016/j.proci.2014.05.130
1540-7489/© 2014 The Combustion Institute. Published by Elsevier Inc. All rights reserved.

enhance the ignitability and flame speed when added to methane, and the promoting effects improved progressively with increase in ethylene concentration [3]. Such a gradual promotion has profound implications on the combustion control strategies of practical devices. In addition, valuable insights into the fundamental kinetics and combustion behavior of HC's can be obtained by studying binary mixtures containing C_2H_4. All these factors provide the necessary motivation for measurement of flame speeds of alkane–ethylene mixtures.

Given the hierarchical nature of chemical kinetics mechanisms, blending a higher- and a lower-order HC (alkene and alkane) provides a stringent assessment for identifying model deficiencies. An in-depth, side-by-side comparison on the effects of blending ethane and ethylene (collectively referred to as C_2H_x from here on) with methane is conducted here, and the paper is organized as follows. First, flame speed studies from the literature that focused on blending ethylene with alkanes are reviewed. The experimental apparatus and measurement techniques are then explained in detail, followed by validation of the kinetics model for C_2H_x. Flame speeds of the CH_4/C_2H_x blends are then presented. Finally, the various enhancement pathways of CH_4 flame speeds with C_2H_x addition are analyzed, with emphasis on discerning the relative chemical kinetic, thermal, and diffusive effects.

2. Background literature

Not many studies have been presented in the literature regarding flame speeds of binary alkane/C_2H_x blends. A few of these studies are discussed next. Hirasawa et al. [4] measured laminar flame speeds of binary blends of ethylene in n-butane and in toluene using a counter-flowing, twin-flame setup. The flame speeds of the blends did not follow a simple mole fraction-based weighted average of the parent fuels. They proposed a semi-empirical flame-temperature-based mixing rule for predicting flame speeds of blends as the kinetic coupling between n-butane and ethylene was minimal. Liu et al. [3] observed monotonic increases in flame speeds of methane with ethylene addition for a wide range of equivalence ratios from 0.8 to 1.3 and over a wide range of pressures from 1- to 10-atm. It was also shown that methane oxidation chemistry was a subset of ethylene chemistry through a skeletal mechanism reduction method. This close connection between CH_4 and C_2H_4 chemistry further highlights the need to measure CH_4/C_2H_4 flame speeds from a hierarchical standpoint of mechanism development and validation.

Lowry et al. [5] measured the laminar flame speeds of 80/20 and 60/40 blends (by volume) of CH_4/C_2H_6 over a wide range of conditions. Blending enhanced the flame speeds of CH_4 and made the flames less susceptible to flame instabilities. However, insights on the reasons for augmentation of flame propagation rates were not provided in either the Liu et al. [3] or Lowry et al. [5] papers. The present study specifically addresses the flame speed enhancement effects of methane with C_2H_x addition. The objectives of this study were twofold- (1) to determine the primary mechanism of flame speed enhancement (thermal, kinetic, or diffusive) of methane with C_2H_x addition; and, (2) to provide a comparative assessment on the impacts ethylene and ethane addition have on the flame speeds of methane and to systematically analyze the reason(s) for the vastly different enhancement rates between the two C_2H_x compounds.

3. Experimental setup and procedure

Flame speeds of spherically expanding flames were measured using the cylindrical vessel described in Krejci et al. [6]. The stainless steel bomb has an inner diameter of 32 cm and an internal length of 28 cm. A z-type schlieren setup was used in conjunction with a high-speed camera (Photron Fastcam SA1.1) to record the flame propagation event. The flame images were processed using a fully automated, MATLAB-based edge-detection code (developed in-house). The test mixtures were prepared using the method of partial pressures, and all consumable gases were of ultra-high-purity grade. Also, the mixtures were allowed to homogenize inside the vessel for 30 min prior to ignition.

Flames up to 12.7 cm (diameter) can be measured under near-constant-pressure conditions (2% increase during the usable part of the experiment) as confirmed by the pressure trace from a high-frequency, dynamic pressure transducer installed inside the vessel (see de Vries et al. [7] for example). Nevertheless, despite the constant-pressure condition, the flame speeds of outwardly propagating flames are still affected by ignition and wall-confinement (induced by finite chamber size) effects [8]. To account for these non-idealities, the flame speed values reported herein are extracted only for flame sizes, r_f/r_w (flame radius normalized by vessel radius), ranging between 0.12 and 0.3 [8]. Given the large diameter of the vessel, this size range corresponds to flame diameters between 3.8 and 9.5 cm. Such a size restriction assures that the measured propagation speeds agree closely with those of an unconfined flame, and do not require any additional flow correction since compression-induced burnt gas motion behind the flame is absent. Sample laminar flame images from the schlieren method for the conditions in this paper are provides in the Supplemental Material.

Spherically expanding flames require extrapolation to zero stretch rate for the unburnt laminar flame speed of a planar flame front (e.g., the linear Markstein relationship Eqs. (1), (2)). More-sophisticated nonlinear relationships (NM-I: Eq. (3); NM-II: Eq. (4)) have been proposed over the conventional linear Markstein relationship to account for variations in Lewis number (Le) [9]. It was shown by Chen [9] that failure to use the appropriate nonlinear model could result in significant over prediction of flame speeds and Markstein lengths, for example, by 35% and 283% respectively, for methane/air at $\phi = 1.34$ (by using the linear correlation). The choice of the appropriate nonlinear model for outwardly propagating flames depends on the Lewis number of the test mixture. NM-I is used for near-unity and positive Lewis numbers (Le $\gg 1$), and NM-II is used when Le < 1. Figure 1 shows an example of flame speed as a function of flame stretch (from data measured herein) accounting for non-ideal effects and incorporating the nonlinear extrapolation techniques. In Eqs. (1)–(4), $L_{m,b}$ is the burnt-gas Markstein length, r_f is the flame radius, S_b is the stretched burned-gas flame speed, and S_b^0 is the un-stretched, burned laminar flame speed. The unburnt, unstretched flame speed is obtained by multiplying S_b^0 with the density ratio of burnt to unburnt gas (from Equilibrium).

$$\text{Linear Markstein relation}: S_b = S_b^0 - L_{m,b}\kappa \qquad (1)$$

$$\text{Stretch rate}: \kappa = (2/r_f)dr/dt \qquad (2)$$

$$\text{NM-I}: S_b = S_b^0 - S_b^0 L_{m,b}(2/r_f) \qquad (3)$$

$$\text{NM-II}: \ln(S_b) = \ln(S_b^0) - S_b^0 L_{m,b}[2/(r_f S_b)] \qquad (4)$$

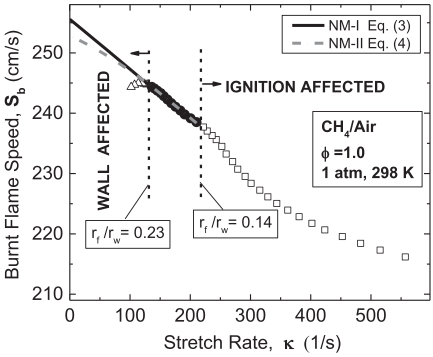

Fig. 1. Flame speed variation with stretch rate. Filled symbols are usable data for nonlinear interpolation, and open symbols are affected by non-ideal effects.

4. Uncertainty analysis

Bias or systematic error (B_{SL}) and random uncertainty (P_{SL}) form the total uncertainty, $U_{SL} = (B_{SL}^2 + P_{SL}^2)^{0.5}$. The systematic error is defined as $B_{SL} = (\sum_i(\partial S_{L,u}(x_i)/\partial x_i)u_i)^{0.5}$, where x_i is the independent variable (i.e., p, T) that affects the flame speed, and u_i is the precision with which it can be measured. Since the mixtures were prepared using the method of partial pressures, uncertainty in pressure manifests as uncertainty in equivalence ratio. Herein, u_ϕ and u_T are the manufacturer-specified precisions for the pressure gauge and the thermocouple, respectively. A functional relationship for flame speed of the form, $S_{L,u}(x_i) = S_{L,u}(\phi, T) = ((\sum_{j=0}^{4} a_j\phi^j)(T/298)^{\sum_{j=0}^{3} b_j\phi^j}$, was derived for each fuel using PREMIX calculations, and was then used to estimate the derivative of $S_{L,u}$ with respect to ϕ and T. The bias error was then estimated for the different ϕ for all blends tested herein.

The random or precision uncertainty was calculated from several repeats of a fixed condition and is defined as $P_{S_L} = ((t_{M-1,1.95\%} S_{SL})/\sqrt{M}$, where M is the sample size, S_{SL} is the sample standard deviation, and $t_{M\text{-}1,95\%}$ is the two-tailed inverse of the Student t-distribution with M-1 degrees of freedom and a 95% confidence interval. The precision uncertainty was calculated using 29 repeats of methane/air mixtures at $\phi = 1$ from an earlier study, and was estimated to be 0.27 cm/s. Such a rigorous approach resulted in a maximum uncertainty of ±1.05 cm/s for the mixtures tested herein.

5. Chemical kinetics model validation

Unburnt, unstretched laminar flame speeds were obtained using PREMIX from Chemkin using AramcoMech 1.3 [10]. Multi-component transport properties and thermal diffusion (Soret effect) were included, and the simulations converged over 3000 grid points with the burnt-gas temperatures being within 5 K of their adiabatic flame temperatures (T_{ad}). This kinetics mechanism was validated for the purposes herein by comparing it with measured laminar flame speeds of pure C_2H_x-air mixtures from several different sources: literature data when available, recent data from the present authors, and new data over a selective range of conditions. New laminar flame speed data were obtained for pure C_2H_4 at 1 atm; pure C_2H_2 at 1 and 2 atm, and some select data for ethane at 1 atm to verify the repeatability of the ethane measurements from Lowry et al. [5]. Tables listing the new data (flame speeds, Markstein lengths and numbers) are provided in Supplemental Material. The mechanism has been compared with methane-air data in Lowry et al. [5] and is not elaborated upon herein for brevity.

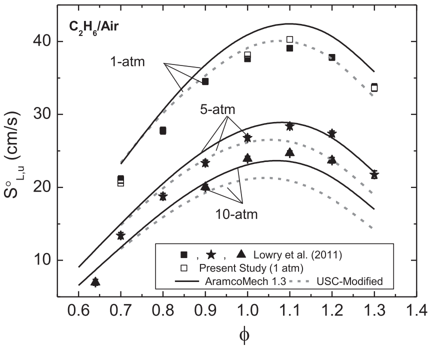

Fig. 2. Ethane flame speeds at 1, 5, and 10 atm. Good agreement is seen between the ArmcoMech mechanism predictions and the measured data, particularly at the higher pressures.

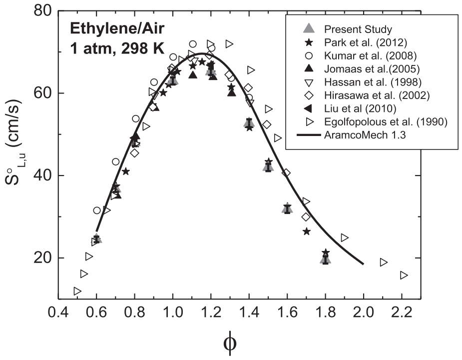

Fig. 3. Measured 1-atm flame speeds of pure ethylene/air mixtures validated with literature data. (See above-mentioned references for further information.)

Figure 2 compares the authors' past and current experimental data for ethane against model predictions at various pressures. Note that the previously published ethane dataset from Lowry et al. [5] was verified with the new data taken in the present study (open symbols in Fig. 2), and good repeatability is evident. High-pressure ethane flame speeds were compared with other available ethane results from the literature in Lowry et al. [5], so it is not repeated here. In a recent C2 laminar flame speed study, interestingly, Park et al. [11] replaced the rate coefficients of two important reactions (1) $C_2H_5 + M = C_2H_4 + H + M$; and (2) $H + C_2H_5 = CH_3 + CH_3$ in the USC mechanism [12] with those from the AramcoMech 1.3 mechanism to correct for the over-prediction of ethane flame speeds at 1 atm. This modified USC mechanism's predictions are also included in Fig. 2. While the different rate coefficient values result in better agreement at 1 atm, the unaltered AramcoMech follows the measured data more closely at elevated pressures. Hence, changing the rate constants of a few reactions to match the data at 1 atm does not necessarily make the model better at all conditions. While improvements are still needed at 1 atm for the mechanism employed herein, it nonetheless performs acceptably well over a relatively wider range of pressures, stoichiometries, and fuel blends.

Additionally, the AramcoMech 1.3 model was compared against new and existing laminar flame speeds of ethylene (Fig. 3) and acetylene (Fig. 4). Good agreement is seen between the new data herein and those reported in the literature. In Fig. 4, the acetylene data from the present study agrees particularly well with the data from Jomaas et al. [14]. The kinetics model successfully captures the experimental data at fuel-lean conditions for both fuels, but over predicts the data for the fuel-rich cases. Changing the branching ratios of $C_2H_2 + O = HCCO + H$ and $C_2H_2 + O = CH_2 + CO$ from 0.42:0.58, presently used in the AramcoMech model, to 0.8:0.2 (from the USC mechanism) was found by Park and coworkers to reduce acetylene flame speeds by 5 cm/s for fuel-rich mixtures at 1 atm [11]. However, such changes were not incorporated in the mechanism for the reasons stated previously, and the AramcoMech 1.3 model can be assumed to be sufficiently validated for the purpose of the present study.

It is imperative to point out that the kinetics model validation was performed elsewhere [10] using more extensive and comprehensive datasets from various experimental facilities such as burners, shock tubes, and flame speed bombs. The authors are aware of the pitfalls of using flame speed measurements for model validation. First, the non-linear extrapolation techniques are first-order accurate (to the inverse of the flame radius at large flame radius). Chen [9] provided guidelines on the choice of a flame speed model for mixtures characterized by non-unity Lewis numbers by minimizing the residual between the various model estimates (linear, NM-I, and NM-II) and 'a detailed model' that is valid for both large and small flame radii. These guidelines have been used in this study for the appropriate model selection (see Section 3 for further details). Second, radiation-associated heat losses can significantly alter the burned gas density in outwardly propagating flames. To that effect, Santner et al. [15] have showed through detailed simulations that the reductions in flame speeds due to radiative losses were pronounced only at elevated pressures. The measurements herein were obtained at ambient conditions, and hence the authors are convinced that radiation-associated losses are only minor and do not change the conclusions from this study. These detailed models and assumptions are necessary in producing high-fidelity datasets for kinetics model validation, and that conscious efforts have been made to incorporate these recent developments into the measurements from this study.

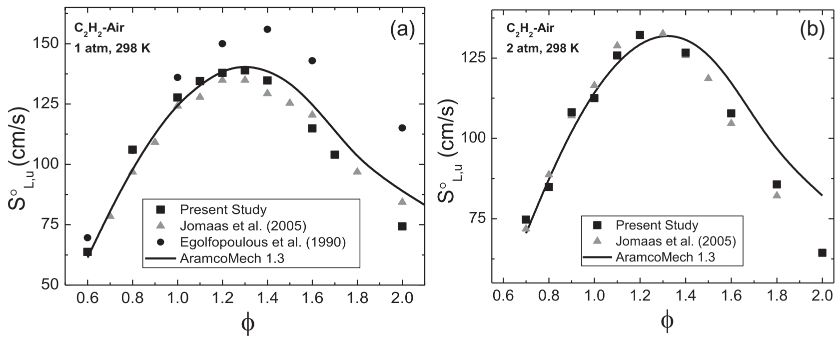

Fig. 4. Laminar flame speeds of acetylene in air (a) 1 atm (b) 2 atm and comparison with the chemical kinetics mechanism.

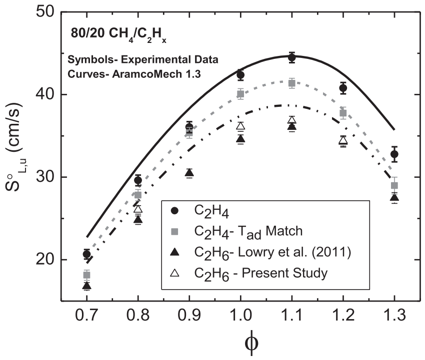

Fig. 5. Laminar flame speeds for the 80/20 CH_4/C_2H_x blends. Symbols are experimental data and curves are kinetics model predictions.

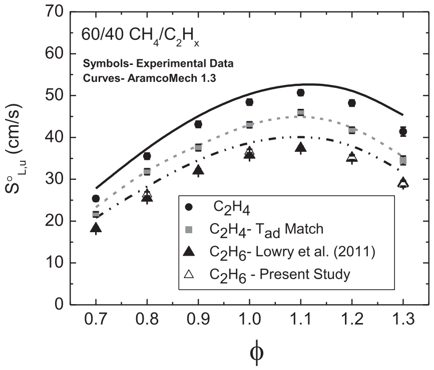

Fig. 6. Laminar flame speeds for the 60/40 CH_4/C_2H_x blends. Symbols are experimental data and curves are kinetics model predictions.

6. Laminar flame speeds of CH_4/C_2H_X blends

Figures 5 and 6 show the laminar flame speeds of CH_4/C_2H_x blends at two different mixing ratios, 80/20 and 60/40 by volume. The blending ratios for the CH_4/C_2H_x fuel mixtures were chosen to agree with the blends utilized in the earlier ethane study [5] to perform a comparative assessment on the C_2H_x addition to methane. All experiments were performed at ambient initial conditions. As seen with ethane, ethylene addition enhances the flame speeds of methane at all equivalence ratios but at much higher enhancement rates than for C_2H_6. The original CH_4/C_2H_6 data from Lowry et al. [5] were repeated in a few new experiments at the same conditions (shown as open symbols), and the new data agree with the earlier measurements. The model over predicts the flame speeds at all equivalence ratios for ethane-based mixtures. The agreement is better for CH_4/C_2H_4, but improvements are still needed for the fuel-rich cases.

From Figs. 5 and 6, one can see that, as expected, the laminar flame speeds for the blends containing ethylene are higher than those with ethane. It is of interest to determine whether the difference is due to adiabatic flame temperature (T_{ad}) effects or due to the chemical kinetics. Noting the higher flame temperatures of the ethylene-based mixtures (see Supplementary Material), a mixture was formulated so that a fuel blend containing ethylene had the same flame temperatures as a corresponding blend containing ethane. Such a mixture was formulated by adding excess nitrogen to CH_4/C_2H_4 such that T_{ad} of the resulting mixture was within 5 K of that of CH_4/C_2H_6 (in air) for the same equivalence and fuel blending ratios. Nitrogen-rich flame speeds of both 80/20 and 60/40 blends of CH_4/C_2H_4 were measured over the same range of ϕ of the blends measured earlier using standard air. The measured flame speeds of the ethylene blends in air containing excess nitrogen are also shown in Figs. 5 and 6. The resulting flame speeds decreased significantly for the diluted blends, for example by 10 cm/s for the 60/40 CH_4/C_2H_4 mixtures in Fig. 6. Also, the agreement between the measured data and the model predictions improved for these T_{ad}-matched blends.

7. Discussion

Flame-speed-enhancing effects of C_2H_x addition to CH_4 can be categorized into thermal, kinetic, and diffusive effects [16,17]. The contribution of each effect can be modeled as

$$S^0_{L,u} \sim (\alpha Le)^{1/2} \exp(-T_a/2T_{ad}) \tag{5}$$

The first term on the right-hand side represents the diffusive effect (which is the product of the mixture thermal diffusivity, α, and the Lewis number of the blend). The second term is the Arrhenius factor which represents the combined contribution of the activation temperature ($T_a = E_a/R$; where, E_a is the global activation energy and R is the universal gas constant) and the adiabatic flame temperature. The two terms represent the kinetic and thermal pathways, respectively. Lewis numbers for single-component fuels, for sufficiently off-stoichiometric cases, are defined as the ratio of the mixture thermal–to-mass diffusivities of the deficient species into the diluent. For HC blends, two definitions, namely, heat-release-based values ($\mathrm{Le_q}$) and a volumetric-weighted-scheme ($\mathrm{Le_v}$) are typically used, as reviewed by Bouvet et al. [18] (and references therein). The heat-based number $\mathrm{Le_q}$ is computed as the weighted average based on the non-dimensional heat of reactions of the parent fuels, while $\mathrm{Le_v}$ is a mole-fraction-weighted scheme between the parent fuels in the blend. The two definitions are shown in Fig. 7 for CH_4/C_2H_x blends at two different ϕ, one lean (0.7) and one rich (1.3). There are noticeable differences between the two definitions for $\phi = 0.7$, although agreement is better at $\phi = 1.3$. Also, Le for lean (rich) CH_4/C_2H_4-blends are lower (higher) than those of CH_4/C_2H_6-blends. Nevertheless, the overall trends in Le are the same irrespective of the definition.

The activation energy E_a ($E_a = -2R[\partial(\rho S^0_L)/\partial(1/T_{ad})]_{\phi,p}$) is defined as the slope of the mass burning flux and the inverse adiabatic flame temperature at constant ϕ, p. The mass burning flux can be varied by changing the diluent concentration or by preheating the unburnt gas (or numerically varying unburnt gas temperature in PREMIX as done herein), but the diluent approach also changes the reactant concentration [19]. E_a for pure ethylene, estimated herein from chemical kinetics simulations, agreed well with the experimentally determined values by Kumar et al. [2] (not shown here).

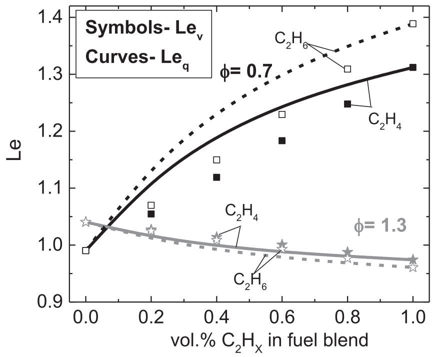

Fig. 7. Lewis number variation for fuel-rich and lean cases of CH_4/C_2H_x fuel blends. Smooth transition of Le between the parent fuels is evident. Solid curves and closed symbols represent the ethylene-based mixtures, while the dashed curves and open symbols represent the ethane-based mixtures.

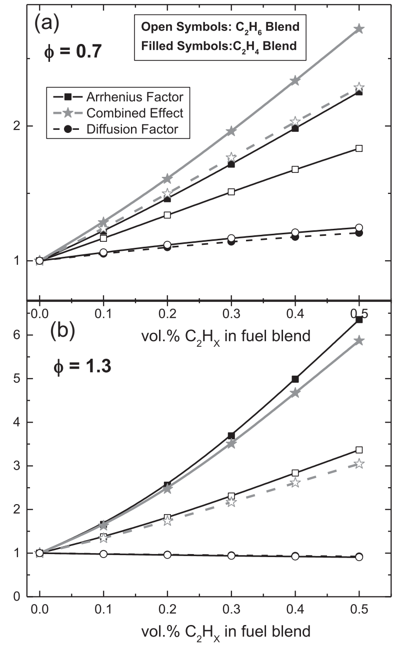

Fig. 8. Arrhenius and diffusive effects of C_2H_x addition to methane for (a) $\phi = 0.7$ and (b) $\phi = 1.3$. The Arrhenius factor dominates the diffusive effects at both equivalence ratios. Legends are the same for both the figures. All factors are normalized by those of pure methane.

Figure 8 shows the variations in Arrhenius and diffusion factors (from Eq. (5)) for CH_4/C_2Hx blends at different levels of C_2Hx and at two different ϕ, all normalized by those of pure methane (denoted by asterisk-$*$). The Arrhenius factor ($\exp(-T_a/2T_{ad})/\exp(-T^*_a/2T^*_{ad})$) always plays a dominant role when compared to the diffusive factor ($(\alpha Le)^{1/2}/(\alpha^* Le^*)^{1/2}$) regardless of the equivalence ratio. The enhancement rates have a positive (negative) sensitivity with respect to the diffusion factor when the mixtures are fuel-lean (fuel-rich). This behavior is consistent with trends in Le variation seen in Fig. 7. Thus, the primary mechanism for flame speed enhancement of methane with C_2Hx addition is via the thermal and kinetic pathways (Arrhenius effect).

Next, the vastly different enhancement rates of ethylene when compared to ethane in CH_4/C_2H_x blends are investigated. Eq. (5) can be differentiated to determine the sensitivity of each pathway on the overall enhancement or inhibition of flame speeds. Thus,

$$\frac{1}{S^{\circ}_{L,u}}\frac{dS^{\circ}_{L,u}}{dx} = \frac{1}{2\alpha Le}\frac{d(\alpha Le)}{dx} - \frac{1}{2T_{ad}}\frac{dT_a}{dx} + \frac{T_a}{2T^2_{ad}}\frac{dT_{ad}}{dx} \tag{6}$$

where x is the volume fraction of C_2H_x in the fuel blend.

Diffusive effects are represented by the first term on the right of Eq. (6). The kinetic (activation temperature) and the thermal (flame temperature) contributions are the last two terms, respectively. The kinetic and thermal effects are coupled and hence are usually grouped as the Arrhenius effect (shown earlier). Sensitivity analysis was conducted at two different mixture strengths (Figs. 9 and 10) over a wide range of blending ratios (10–50% C_2H_x in the blend). All three pathways have a positive sensitivity (or enhancing effect) on the flame speeds of CH_4/C_2H_x blends at $\phi = 0.7$. The diffusion effect, however, has a negative sensitivity (or inhibiting effect) for the fuel-rich mixtures. For CH_4/C_2H_x mixtures, the dominant mechanism of flame speed enhancement is through the reduction of the activation energy, i.e. the kinetic effect. For lean ethane-based mixtures, the diffusive pathway has a stronger influence on the enhancement rate than the thermal effect. This behavior is consistent with the fact that the T_{ad} of CH_4/C_2H_6 does not increase appreciably with ethane addition. However, for lean ethylene blends, the thermal effect is stronger than the diffusion effect, and the thermal effect becomes comparable to the kinetic effect as the C_2H_4 concentration is increased (as the activation energy asymptotes to E_a for pure ethylene). Furthermore, the kinetic effect of CH_4/C_2H_4 is higher (lower) than that of C_2H_6-doped blends for rich (lean) mixtures.

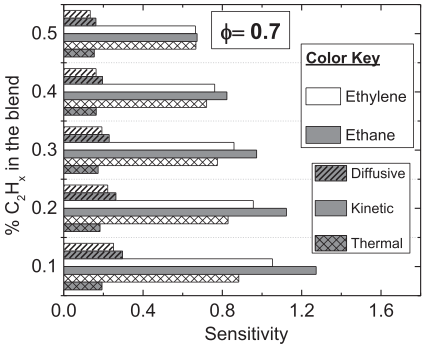

Fig. 9. Sensitivity of CH_4/C_2H_x flame speeds to diffusive, thermal, and kinetic effects at $\phi = 0.7$. The two fuel blends are pattern-coded. Different patterns are used to distinguish between the various pathways.

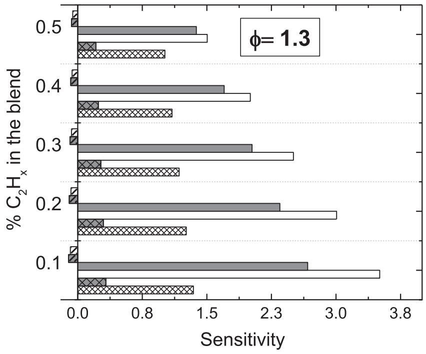

Fig. 10. CH_4/C_2H_x flame speed sensitivities for $\phi = 0.7$. The legends are the same as in Fig. 9.

The conclusions drawn thus far can be used to explain the difference in flame speeds between the N_2-diluted C_2H_4 mixtures and the corresponding C_2H_6-based blends (Figs. 5 and 6). Though the thermal pathway was suppressed by matching the flame temperatures, kinetic and diffusive effects were still present and had a net positive sensitivity on the flame speeds. Sensitivity analysis also validates the earlier hypothesis that the Arrhenius effect is the dominant pathway of flame speed enhancement of CH_4 with C_2H_x addition.

8. Summary

A comparative study on the enhancement of laminar flame speeds of methane with C_2H_x addition was conducted. Laminar flame speeds of binary blends of methane with ethane or ethylene were measured using the spherically expanding flame technique. Care was taken to ensure that the measured flame speeds were not affected by ignition or geometric-confinement effects. Nonlinear extrapolation for flame stretch was incorporated to estimate the planar flame speeds. The kinetics mechanism was validated using new and existing experimentally measured flame speeds of ethane, ethylene, and acetylene. Good agreement between the kinetics model predictions and the measurements at fuel-lean conditions and slight over prediction for the fuel-rich cases were observed.

Two binary fuel blends, 80/20 and 60/40 (by volume), of CH_4/C_2H_x were measured. Blends with ethylene yielded higher flame speeds when compared to those containing ethane. Rigorous analysis based on first principles revealed that the enhancement of flame speeds of methane with C_2H_x addition was primarily an Arrhenius effect rather than a diffusive one. Sensitivity analysis showed that the dominant mechanism of flame speed enhancement of the CH_4/C_2H_x blends was through the reduction of the global activation energy (i.e., a kinetic effect). The diffusion effect had a positive (negative) sensitivity for lean (rich) ϕ for the different blends. Flame temperature had a stronger effect than the diffusive pathway for ethylene-containing mixtures, but was comparable to the diffusive effect for ethane-based mixtures.

Appendix A. Supplementary material

Supplementary data associated with this article can be found, in the online version, at http://dx.doi.org/10.1016/j.proci.2014.05.130.

References

[1] C.V. Naik, A.M. Dean, *Combust. Flame* 145 (1–2) (2006) 16–37.
[2] K. Kumar, G. Mittal, C.J. Sung, C.K. Law, *Combust. Flame* 153 (3) (2008) 343–354.
[3] W. Liu, A.P. Kelley, C.K. Law, *Combust. Flame* 157 (5) (2010) 1027–1036.
[4] T. Hirasawa, C.J. Sung, A. Joshi, Z. Yang, H. Wang, C.K. Law, *Proc. Combust. Inst.* 29 (2002) 1427–1434.
[5] W. Lowry, J. de Vries, M. Krejci, E. Petersen, Z. Serinyel, W.K. Metcalfe, H. Curran, G. Bourque, *J. Eng. Gas Turb. Power* 133 (9) (2011), 091501-1-091501-9.
[6] M.C. Krejci, O. Mathieu, A.J. Vissotski, S. Ravi, T.G. Sikes, E.L. Petersen, A. Kérmonès, W. Metcalfe, H.J. Curran, *J. Eng. Gas Turb. Power* 135 (2) (2013), 021503-1-021503-9.
[7] J. de Vries, W.B. Lowry, Z. Serinyel, H.J. Curran, E.L. Petersen, *Fuel* 90 (1) (2011) 331–338.
[8] M.P. Burke, Z. Chen, Y. Ju, F.L. Dryer, *Combust. Flame* 156 (4) (2009) 771–779.
[9] Z. Chen, *Combust. Flame* 158 (2) (2011) 291–300.
[10] W.K. Metcalfe, S.M. Burke, S.S. Ahmed, H.J. Curran, *Int. J. Chem. Kinet.* 45 (10) (2013) 638–675.
[11] O. Park, P.S. Veloo, F.N. Egolfopoulos, *Proc. Combust. Inst.* 34 (2013) 711–718.
[12] H. Wang, X. You, A.V. Joshi, S.G. Davis, A. Laskin, F. Egolfopoulos, C.K. Law, USC Mech Version II. High-Temperature Combustion Reaction Model of $H_2/CO/C_1–C_4$ Compound, (2007), <http://www.ignis.usc.edu/USC_Mech_II.htm>.
[13] M.I. Hassan, K.T. Aung, O.C. Kwon, G.M. Faeth, *J. Propul. Power* 14 (4) (1998) 479–488.
[14] G. Jomaas, X.L. Zheng, D.L. Zhu, C.K. Law, *Proc. Combust. Inst.* 30 (2005) 193–200.
[15] J. Santner, F.M. Haas, Y. Ju, F.L. Dryer, *Combust. Flame* 161 (1) (2014) 147–153.
[16] F. Wu, A.P. Kelley, C. Tang, D. Zhu, C.K. Law, *Int. J. Hydrogen Energy* 36 (20) (2011) 13171–13180.
[17] C.L. Tang, Z.H. Huang, C.K. Law, *Proc. Combust. Inst.* 33 (2011) 921–928.
[18] N. Bouvet, F. Halter, C. Chauveau, Y. Yoon, *Int. J. Hydrogen Energy* 38 (14) (2013) 5949–5960.
[19] K. Kumar, C.J. Sung, *Combust. Flame* 151 (1–2) (2007) 209–224.